Research Square

Preprints are preliminary reports that have not undergone peer review.
They should not be considered conclusive, used to inform clinical practice,
or referenced by the media as validated information.

Chidamide reprograms AML-associated macrophages via HDAC3 inhibition to boost CD8+ T cell immunity

Zhili Tan
Southern Medical University
Ziyi Liang
Southern Medical University
Xiaoning Li
Southern Medical University
Yujie Zhang
Southern Medical University
Yuhua Li
Southern Medical University
Yaling Zheng
Southern Medical University
Rui Huang
huangruichn8317@smu.edu.cn
Southern Medical University

Research Article

Keywords: acute myeloid leukemia, macrophages, histone deacetylase inhibition, immunoepigenetics, chidamide

Posted Date: November 20th, 2026

DOI: https://doi.org/10.21203/rs.3.rs-11589394/v1

License: This work is licensed under a Creative Commons Attribution 4.0 International License.
Read Full License

Additional Declarations: No competing interests reported.

Title

Chidamide reprograms AML-associated macrophages via HDAC3 inhibition to boost CD8$^+$ T cell immunity

Author information

Zhili Tan[1,2,#], Ziyi Liang[1,2,#], Xiaoning Li[1,2,#], Yujie Zhang[1,2], Yuhua Li[1,2], Yaling Zheng[1,2]*, Rui Huang[1,2]*

Affiliations:

[1]Zhujiang Hospital of Southern Medical University, Department of Hematology, Guangzhou, Guangdong, China.

[2]Guangdong Engineering Research Center of Precision Immune Cell Therapy Technology.

# Contributed equally.

*Corresponding author

Author Emails:

Zhili Tan: tzl18992554303@smu.edu.cn

Ziyi Liang: liangziyi@smu.edu.cn

Xiaoning Li: lxndexyw123@smu.edu.cn

Yujie Zhang: zhangxiaosi@smu.edu.cn

Yuhua Li (Corresponding Author): lyh2891@smu.edu.cn

Yaling Zheng (Corresponding Author): yling@smu.edu.cn

Rui Huang (Corresponding Author): huangruichn8317@smu.edu.cn

Abstract

Acute myeloid leukemia (AML) is a highly aggressive hematological malignancy frequently associated with relapse and therapeutic resistance. AML-associated macrophages (AAMs) within the microenvironment play an important role in immune escape. Chidamide, a histone deacetylase (HDAC) inhibitor, has been reported to activate $CD8^+$ T cells to exert anti-tumor effects. However, its effect on AAMs remains unclear. The present study aimed to investigate the effects of chidamide on AAMs and the underlying mechanisms. Chidamide treatment conferred an immunologically activated phenotype on AAMs, characterized by upregulated expression of antigen-presenting molecules, pro-inflammatory cytokines, and chemokines. Moreover, chidamide reversed the suppressive effect of AAMs on the proliferation of co-cultured $CD8^+$ T cells. In vivo, chidamide treatment significantly decreased leukemia burden and polarized AAMs towards the M1 phenotype. Mechanistically, chidamide inhibited HDAC3, leading to enhanced H3K27 acetylation. Integrated multi-omics analysis of RNA-seq, ATAC-seq, and CUT&Tag-seq revealed that chidamide upregulated FOSL2 expression, which in turn activated the TNF-α/NF-κB signaling pathway. FOSL2 was found to directly bind to the TNF promoter, thereby driving TNF-α/NF-κB activation. Collectively, our findings demonstrate that chidamide reprograms immunosuppressive AAMs into an immunologically activated phenotype via selective HDAC3 inhibition, thereby eliciting anti-leukemic activity. These findings provide a novel mechanistic rationale for chidamide-based therapy in AML.

Keywords: acute myeloid leukemia, macrophages, histone deacetylase inhibition, immunoepigenetics, chidamide

Introduction

Acute myeloid leukemia (AML) is a highly aggressive hematological malignancy characterized by aberrant proliferation and impaired differentiation of myeloid progenitor cells[1, 2]. Despite substantial advancements in conventional and targeted therapeutic regimens, the clinical prognosis of AML patients remains unsatisfactory, with a 5-year overall survival rate of merely 29%[3–5]. The heterogeneous pathogenesis of AML is driven by diverse genetic mutations, cytogenetic abnormalities, and epigenetic dysregulations, which disrupt normal hematopoiesis and lead to massive accumulation of immature leukemic blasts in the bone marrow and peripheral blood[6]. Disease relapse and therapeutic resistance constitute the primary causes of treatment failure and patient mortality, highlighting an urgent demand for novel and effective therapeutic strategies to improve AML clinical outcomes.

In recent years, aberrant epigenetic regulation has been established as a critical contributor to AML pathogenesis, and drugs targeting epigenetic modifications have been increasingly incorporated into clinical practice for AML treatment[7–9]. Histone acetylation and deacetylation represent core epigenetic modification mechanisms that govern chromatin remodeling and gene transcription[10, 11]. Histone acetyltransferases (HATs) mediate histone acetylation to relax chromatin structure and facilitate gene expression, whereas histone deacetylases (HDACs) remove acetyl groups to induce chromatin condensation and transcriptional repression[12–14]. This reversible epigenetic modulation finely tunes cellular biological behaviors and microenvironmental homeostasis, rendering HDACs promising therapeutic targets for

AML.

Chidamide, a selective HDAC inhibitor, has been validated to exert potent anti-tumor and immunomodulatory effects in hematological malignancies. Existing studies have primarily focused on its direct cytotoxic effects on leukemic cells and synergistic anti-tumor activity with other chemotherapeutic or targeted drugs[15–22]. Beyond direct tumor cell killing, accumulating evidence has confirmed that chidamide remodels the tumor immune microenvironment to enhance anti-tumor immunity, including promoting $CD8^+$ T cell activation, enhancing NK cell-mediated tumor cytotoxicity, and suppressing the immunosuppressive function of myeloid-derived suppressor cells (MDSCs)[23, 24]. However, most current investigations ignore the regulatory effect of chidamide on AML-associated macrophages (AAMs), a key immune component in the AML microenvironment.

Tumor-associated macrophages (TAMs) are central regulators of tumor immune escape and microenvironmental immunosuppression. In the AML bone marrow microenvironment, AAMs undergo dynamic M1/M2 phenotypic polarization, and the immunosuppressive M2-like AAMs facilitate leukemic cell survival, immune evasion, and disease progression[25–27]. Targeting macrophage phenotypic reprogramming has become a promising strategy to reverse tumor immunosuppression, overcome drug resistance, and improve immunotherapy efficacy[28, 29]. Nevertheless, whether chidamide exerts anti-leukemic effects by modulating AAMs immune function and its specific epigenetic regulatory mechanism remains unclear.

Therefore, in the present study, we systematically investigated the effects of chidamide

on macrophage-mediated anti-AML immunity. Herein, we demonstrated that chidamide reprograms immunosuppressive AAMs into an immunologically activated phenotype via selective HDAC3 inhibition and elevated H3K27 acetylation. Mechanistically, chidamide upregulates FOSL2 expression to activate the TNF-α/NF-κB signaling pathway in AAMs, thereby enhancing antigen presentation and pro-inflammatory immune responses. This AAMs remodeling further restores the proliferative and immune function of $CD8^+$ T cells, ultimately suppressing leukemia progression in vivo. Collectively, our findings reveal a novel epigenetic immunomodulatory mechanism of chidamide in AML, providing an innovative mechanistic rationale for expanding its clinical application in AML treatment.

Materials and methods

Cell lines and cell culture

The RAW264.7 and C1498 cell lines were cultured in DMEM, while the MOLM-13 cell line was maintained in RPMI-1640 medium. Both media were supplemented with 10% FBS. All cells were incubated at 37 °C under 5% CO_2 atmosphere.

Cell isolation and culture

Bone marrow-derived macrophages (BMDMs) were isolated from the tibiae and femurs of C57BL/6 mice. Bone marrow cells were flushed out using sterile syringes, resuspended in DMEM supplemented with 10% FBS and 20 ng/mL recombinant mouse M-CSF, and cultured for 7 days for macrophage differentiation. Culture medium was refreshed on day 3 and day 5.

Human bone marrow mononuclear cells (BMNCs) were isolated from clinical

bone-marrow aspirates using human lymphocyte separation medium. Monocytes were further purified with the EasySep Human Monocyte Isolation Kit. To generate AAMs, monocytes derived from AML patients were cultured in RPMI-1640 supplemented with 10% FBS and 20 ng/mL M-CSF for 7 days. For in vitro AAMs induction from healthy donors, monocytes were differentiated in the same medium supplemented with MOLM-13-derived tumor-conditioned medium for 7 days.

Preparation of tumor-conditioned medium (TCM) and establishment of an in vitro AAMs model

AML tumor cells were cultured in serum-free medium for 24 h. Supernatants were collected, centrifuged at 3000 rpm for 10 min, and filtered through a 0.22-μm filter. The filtrate was mixed 1:1 with fresh complete medium to adjust final 10% FBS to yield TCM. RAW264.7 cells were incubated with TCM for 24 h, and BMDMs for 48 h, to establish the AAMs model.

Mice

Five-week-old female C57BL/6 mice were purchased from BesTest Bio-Tech Co., Ltd. (Zhuhai, China). Animals were housed under specific-pathogen-free (SPF) conditions with a 12-h light-dark cycle and free access to food and water. All animal experiments were performed in accordance with institutional guidelines and approved by the Institutional Animal Care and Use Committee of Zhujiang Hospital, Southern Medical University (LAEC-2025-044).

T cell isolation

Spleens harvested from C57BL/6 mice were mechanically dissociated and passed

through a 70-μm cell strainer to obtain single-cell suspensions. $CD8^+$ T cells were purified using the EasySep Mouse $CD8^+$ T Cell Isolation Kit (STEMCELL, cat#19853) and activated with plate-bound anti-CD3/anti-CD28 antibodies in RPMI-1640 containing 10% FBS, 500 IU/mL recombinant human IL-2, 1 × non-essential amino acids, and 1 × β-mercaptoethanol.

BMDM-AAMs and $CD8^+$ T-cell co-culture assay

BMDMs in 48-well plates were differentiated into AAMs and pretreated with chidamide for 48 h. After removing chidamide, CFSE-labeled $CD8^+$ T cells were added at a 2:1 ratio and co-cultured for 72 h. T-cell proliferation was assessed via flow cytometry.

CCK-8 assay

RAW264.7 cells were plated in 96-well plates at a density of 2×10^5 cells per well and treated with serially diluted chidamide; three replicate wells were set for each condition. After 24 h incubation, 10 μL CCK-8 reagent was added to each well, and plates were incubated at 37 °C in the dark for 3 h. Absorbance was measured at 450 nm.

Annexin V/PI assay

RAW264.7 cells were seeded in 12-well plates and exposed to different concentrations of chidamide for 24 h. Apoptosis was evaluated using the Annexin V-APC/PI Apoptosis Detection Kit (Elabscience, cat#E-CK-A221) according to the manufacturer's instructions. After incubation at room temperature in the dark for 20 min, samples were analysed by flow cytometry within 1 h.

Flow cytometry

Cultured cells were harvested and washed with FACS buffer (PBS supplemented with 2% FBS). For mouse spleen and bone-marrow single-cell suspensions, red blood cells were lysed with ACK lysis buffer prior to staining. Cell-surface staining was performed following antibody manufacturer protocols. After two washes with FACS buffer, samples were acquired on a CytoFLEX flow cytometer (Beckman). Data were analysed using FlowJo software. Antibody information is summarized in Supplementary Table S1.

Western blot

Total cellular protein was extracted by lysing cells on ice for 20 min in RIPA lysis buffer. Nuclear protein fractions were prepared using a Nuclear Protein Extraction Kit (Solarbio, cat#EX1470). Protein concentrations were quantified with a BCA protein assay kit. Proteins were separated by SDS-PAGE, transferred onto membranes, and blocked. Membranes were incubated with primary antibodies overnight at 4 °C, followed by HRP-conjugated secondary antibodies for 1 h at room temperature. Immunoreactive bands were visualized using chemiluminescent substrate on a Tanon imaging system. Band intensities were quantified with ImageJ software and normalized to corresponding loading controls. Antibody details are provided in Supplementary Table S1.

Quantitative real-time PCR (qRT-PCR)

Total RNA was isolated using TRIzol reagent (TaKaRa, cat#9109) and reverse-transcribed into cDNA with the Reverse Transcription Master Mix kit (Vazyme,

cat#R323-01). qRT-PCR was run using SYBR Green Premix Pro Taq HS qPCR Kit III (Low Rox Plus) (AG, cat#AG11739) on a Bio-Rad CFX Real-Time PCR System. Gene expression was normalized to *GAPDH*. Relative mRNA levels were calculated using the $2^{-\Delta Ct}$ method, and fold-change values were computed by the $2^{-\Delta\Delta Ct}$ approach. Primer sequences are listed in Supplementary Table S2.

siRNA transfection

Target siRNAs were synthesized by igeBio (Guangzhou, China). Transfection was performed with Lipofectamine RNAiMAX (Invitrogen) as per the manufacturer's recommendations. Knockdown efficiency was validated by qRT-PCR at 24 h post-transfection. siRNA sequences are provided in Supplementary Table S3.

ChIP-qPCR

AAMs differentiated from human bone-marrow-derived monocytes were treated with chidamide. Chromatin immunoprecipitation was carried out using the Magnetic ChIP Kit (Thermo Fisher, cat#26157) following manufacturer protocols. Purified ChIP DNA was subjected to qPCR. FOSL2 binding enrichment at the *Tnf* promoter was calculated as percentage of input DNA (% Input). ChIP-qPCR primers are listed in Supplementary Table S2.

RNA sequencing library preparation

TCM was generated from logarithmically growing C1498 cells. RAW264.7 macrophages were seeded in 10-cm dishes at 5×10^7 cells per dish and incubated overnight. Culture medium was replaced with TCM, and cells were treated with 2.5 μM chidamide for 24 h. Harvested cells were resuspended in serum-free cryopreservation

medium and stored at −80 °C. Samples were shipped on dry ice for RNA-seq, which was performed by Guangzhou Saiqing Biotechnology Co., Ltd. Bioinformatic analysis workflows are described in Supplementary Methods.

ATAC and CUT&Tag sequencing library preparation

Cell treatment conditions were identical to those described for RNA-seq. ATAC-seq services were provided by Hangzhou Xingyuan Future Biotechnology Co., Ltd; CUT&Tag-seq services were performed by NewBlue Gene. Bioinformatic analysis workflows are detailed in Supplementary Methods.

In vivo experiments

To establish the syngeneic AML model, 5×10^5 C1498-LUC cells were injected into each mouse via the tail vein. Leukemia-bearing animals were randomly assigned to vehicle and chidamide-treatment groups. Starting on day 3 post-inoculation, mice received daily oral-gavage administration of vehicle or chidamide (25 mg/kg, MedChemExpress) for 14 consecutive days.

Leukemia burden was monitored using an IVIS Spectrum in-vivo imaging system (PerkinElmer). Ten minutes before imaging, mice received intraperitoneal injection of D-luciferin potassium salt (150 mg/kg; Absin). Mice were anesthetized by isoflurane (RWD, R510-22-10) inhalation during image acquisition. Signal intensity was quantified as average radiance (photons/s/cm²/sr) using the manufacturer's software.

Mice were euthanized by CO_2 overdose via inhalation at pre-defined experimental time-points for tissue collection. For flow-cytometric analysis, spleens and bone marrow were harvested two days after the initiation of drug treatment. Spleens were

mechanically dissociated through 70-μm strainers; bone-marrow cells were flushed from femurs and tibias with sterile PBS. After red-blood-cell lysis, single-cell suspensions were stained with fluorochrome-conjugated antibodies and processed as described in the Flow cytometry section.

Statistical analysis

Flow-cytometry raw data were processed using FlowJo v10.8.1. Data normality was assessed using the Shapiro–Wilk test. Statistical comparisons between two groups were performed with unpaired two-tailed Student's *t*-test; multiple-group comparisons were performed using one-way ANOVA. All quantitative data represent mean ± standard error of the mean (SEM) from at least three independent biological replicates. GraphPad Prism 10.1.2 was used for statistical computation. Significance thresholds were defined as: ns, not significant; $*p < 0.05$; $**p < 0.01$; $***p < 0.001$.

Results

Macrophages in the bone marrow microenvironment of AML patients exhibit an immunosuppressive M2 phenotype

To investigate the differences in macrophages within the bone marrow microenvironment between AML patients and healthy individuals, we performed cell type annotation on the GSE116256 single-cell dataset. UMAP plots revealed differences in the relative abundance and distribution of macrophages between AML patients and healthy individuals (Fig. 1A, Supplementary Fig. 1A). To specifically focus on macrophages, we then reclustered this population into six subpopulations (Fig. 1B, Supplementary Fig. 1B), among which the Macro4 subpopulation was significantly

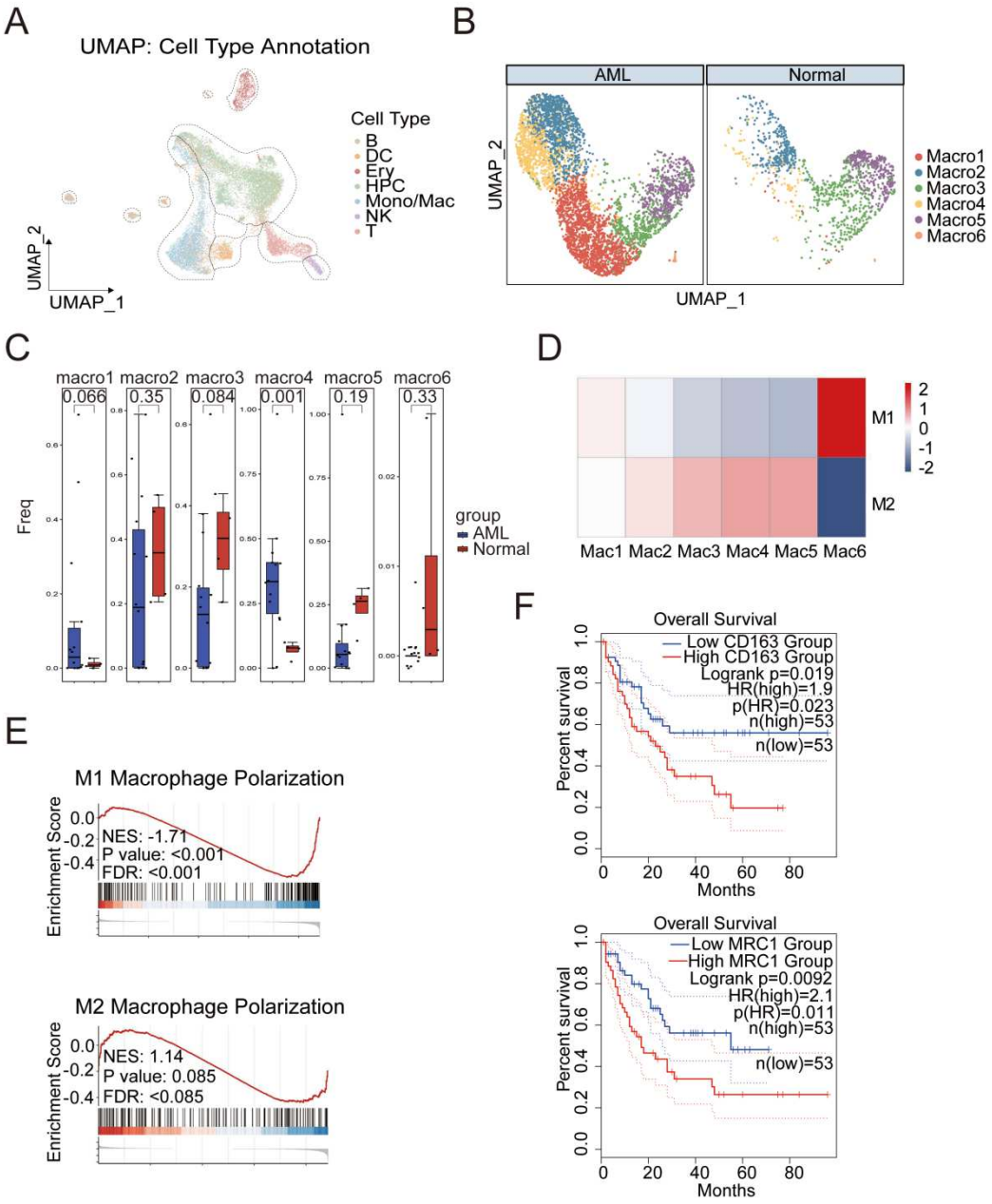


Fig. 1 Increased proportion of M2-type macrophages in AML patients. **A** UMAP plot showing immune cell subpopulations annotated in AML patients and healthy individuals using the GSE116256 dataset. **B** Subcluster results of macrophages obtained after dimensionality reduction and clustering using the UMAP algorithm. **C** Box plot showing differences in the proportions of distinct macrophage subclusters between AML patients and healthy individuals. **D** GSVA heatmap displaying the enrichment of M1/M2 gene sets across various macrophage clusters. **E** GSEA of differential expression of M1/M2-related genes in the AML transcriptome (GSE114868). **F** In the TCGA-LAML cohort, high expression of M2 macrophage marker genes (upper: CD163, lower: MRC1) is associated with poor prognosis

expanded in the AML group (Fig. 1C, $p < 0.01$). GSVA scoring indicated that the

Macro4 subpopulation was more inclined toward an immunosuppressive M2-like polarization state (Fig. 1D). Consistently, an independent bulk transcriptomic dataset (GSE114868) was further analyzed to verify macrophage polarization characteristics in AML. GSEA revealed enrichment of the macrophage M1 polarization gene set in healthy individuals, whereas the M2 polarization gene set showed a trend of enrichment in AML patients (Fig. 1E). Kaplan-Meier survival analysis further demonstrated that high expression of M2 marker genes (*CD206* and *CD163*) was associated with poor prognosis in AML patients (Fig. 1F). Collectively, these findings suggest that macrophages in the AML bone marrow microenvironment tend to exhibit an M2-like immunosuppressive phenotype, which may promote disease progression and influence clinical outcomes.

Chidamide reprograms immunosuppressive M2 macrophages in AML towards an immunocompetent phenotype

We next investigated whether chidamide could reprogram immunosuppressive macrophages within the AML bone marrow microenvironment. To address this issue, we first established an in vitro AAMs model by culturing macrophages in TCM derived from AML cell lines (Fig. 2A). qPCR analysis revealed significant downregulation of M1 macrophage markers (*CD80*, *CCL5*) and prominent upregulation of M2 markers (*CD163*, *IL-10*), confirming the successful construction of an immunosuppressive AAMs model (Fig. 2B).

We subsequently explored whether chidamide could reverse the immunosuppressive phenotype and restore the immune-competent function of AAMs. To exclude the

interference of cytotoxicity and determine the optimal experimental concentrations, we first performed CCK-8 and Annexin V/PI apoptosis assays. The results demonstrated that chidamide at concentrations ranging from 2.5 to 10 μM exerted no obvious cytotoxic or pro-apoptotic effects on RAW264.7 cells (Supplementary Fig. 2A-B), validating the safety of this concentration range for subsequent functional experiments. After chidamide intervention for 24 h, the expression of immune activation-related genes was detected in both RAW264.7 cells and primary BMDMs. qPCR results showed markedly elevated expression of the antigen-presenting molecule *CD80*, pro-inflammatory cytokines (*iNOS*, *TNF-α*, *IL-6*), and chemokines (*CCL4*, *CCL5*) following chidamide treatment (Fig. 2C). Moreover, chidamide dose-dependently upregulated the M1 hallmark marker CD80 in AAMs, further confirming its role in driving AAMs immune activation and phenotypic repolarization (Fig. 2D).

Given that macrophage-mediated immunosuppression primarily impairs anti-tumor T cell immunity, we further investigated whether chidamide-remodeled AAMs could restore $CD8^+$ T cell function. $CD8^+$ T cells isolated from mouse spleens were labelled with CFSE and co-cultured with chidamide-pretreated or untreated BMDMs, with anti-CD3/CD28-activated $CD8^+$ T cells cultured alone serving as the blank control (Supplementary Fig. 3A). Functional assays showed that untreated AAMs significantly inhibited the proliferation of activated $CD8^+$ T cells, whereas chidamide intervention effectively reversed the immunosuppressive capacity of AAMs and rescued $CD8^+$ T cell proliferation (Fig. 2E).

Notably, we further verified this regulatory effect in primary human samples.

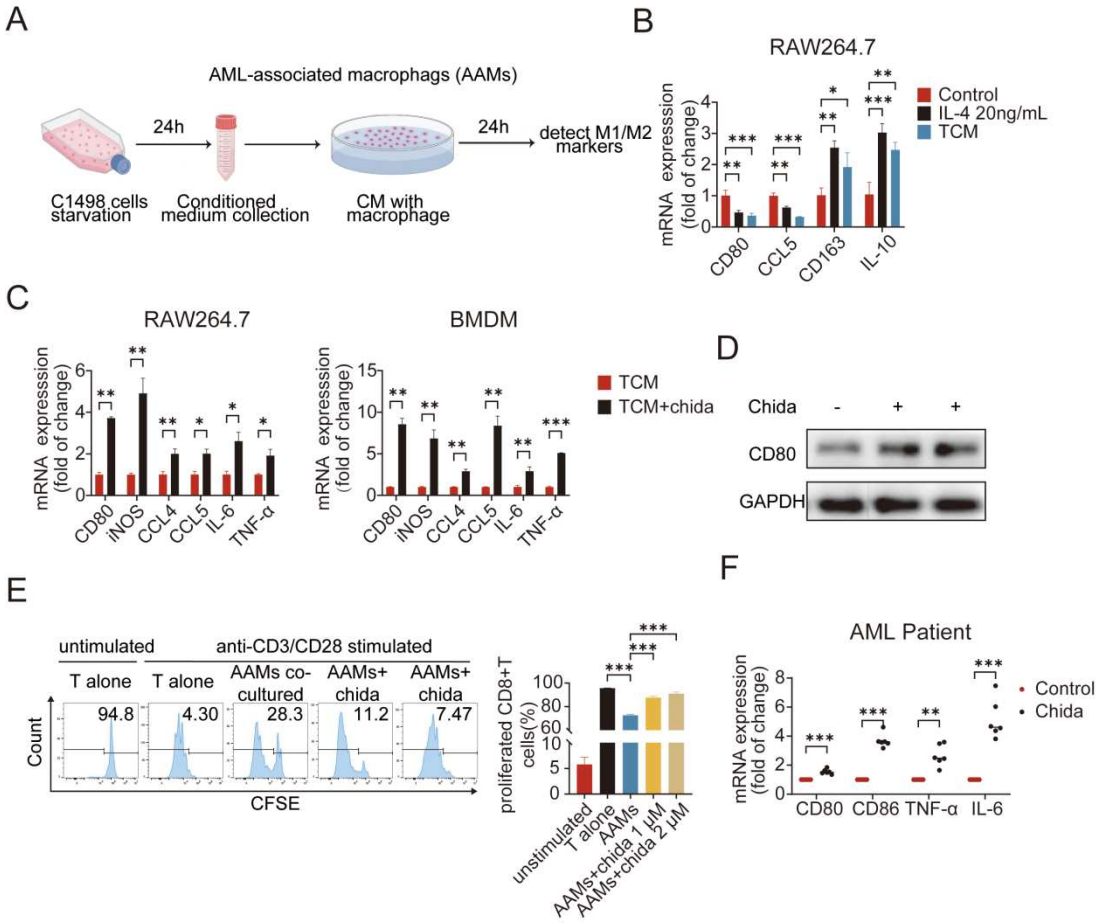


Fig. 2 Chidamide activates immune and inflammatory responses in AAMs. **A** Schematic diagram of the in vitro AAMs model. **B** RAW264.7 cells were induced with IL-4 and TCM for 24 hours, followed by qRT-PCR detection of mRNA expression of *CD80*, *CCL5*, *CD163*, and *IL-10*. **C** mRNA expression of antigen-presenting molecules, chemokines, and pro-inflammatory cytokines in RAW264.7 cells and BMDMs treated with chidamide. **D** Western blot detection of CD80 protein expression(Chidamide:2.5μM,5μM). **E** Left: representative flow cytometry plots showing $CD8^+$ T cell proliferation capacity in co-culture with AAMs with or without chidamide treatment. Right: bar graph showing statistical data. **F** Monocytes isolated from bone marrow mononuclear cells of AML patients were differentiated into macrophages and treated with or without chidamide, followed by mRNA expression analysis of immune- and inflammation-related genes. $*p < 0.05$, $**p < 0.01$, $***p < 0.001$; ns, not significant by paired Student's t-test **B-C, F** or one-way ANOVA with Dunnett's multiple comparisons test **E**

Monocytes isolated from bone marrow aspirates of AML patients were induced into macrophages and treated with chidamide in vitro. Consistent with the results obtained from murine macrophages, chidamide significantly upregulated the expression of immune activation and pro-inflammatory genes in human AML-associated

316 macrophages (Fig. 2F, Supplementary Fig. 3B).

317 **Chidamide promotes macrophage activation and restrains AML**

318 **progression in vivo**

319 Having established that chidamide triggers immune activation of AAMs and reverses
320 their suppression of $CD8^+$ T cells in vitro, we next investigated whether these
321 immunomodulatory effects could be recapitulated in vivo and whether such changes
322 were coupled with attenuated AML progression. A syngeneic AML model was
323 established, and beginning on day 3 after leukemia cell inoculation, mice were
324 administered vehicle or chidamide (25 mg/kg) by oral gavage once daily for 14
325 consecutive days (Fig. 3A).

326 To evaluate early changes in macrophage polarization upon chidamide administration,
327 we prepared single-cell suspensions from bone marrow and spleen at day 2 after
328 treatment initiation and performed flow cytometric analysis. The frequency of $CD80^+$
329 macrophages, a marker of M1 polarization, was markedly elevated in both bone marrow
330 and spleen from chidamide-treated mice relative to vehicle controls (Fig. 3B).

331 We then explored whether chidamide-mediated macrophage M1 polarization correlated
332 with reduced leukemia burden. Bioluminescence imaging was performed on days 5, 9,
333 13, and 17 post C1498-LUC cell engraftment to dynamically monitor leukemia
334 progression. Although leukemia burden increased progressively in both groups,
335 chidamide treatment significantly reduced leukemic burden at days 9 and 13 (Fig. 3C).
336 These results demonstrate that chidamide delays AML progression, particularly at early
337 disease stages. Collectively, chidamide promotes M1 polarization of macrophages in

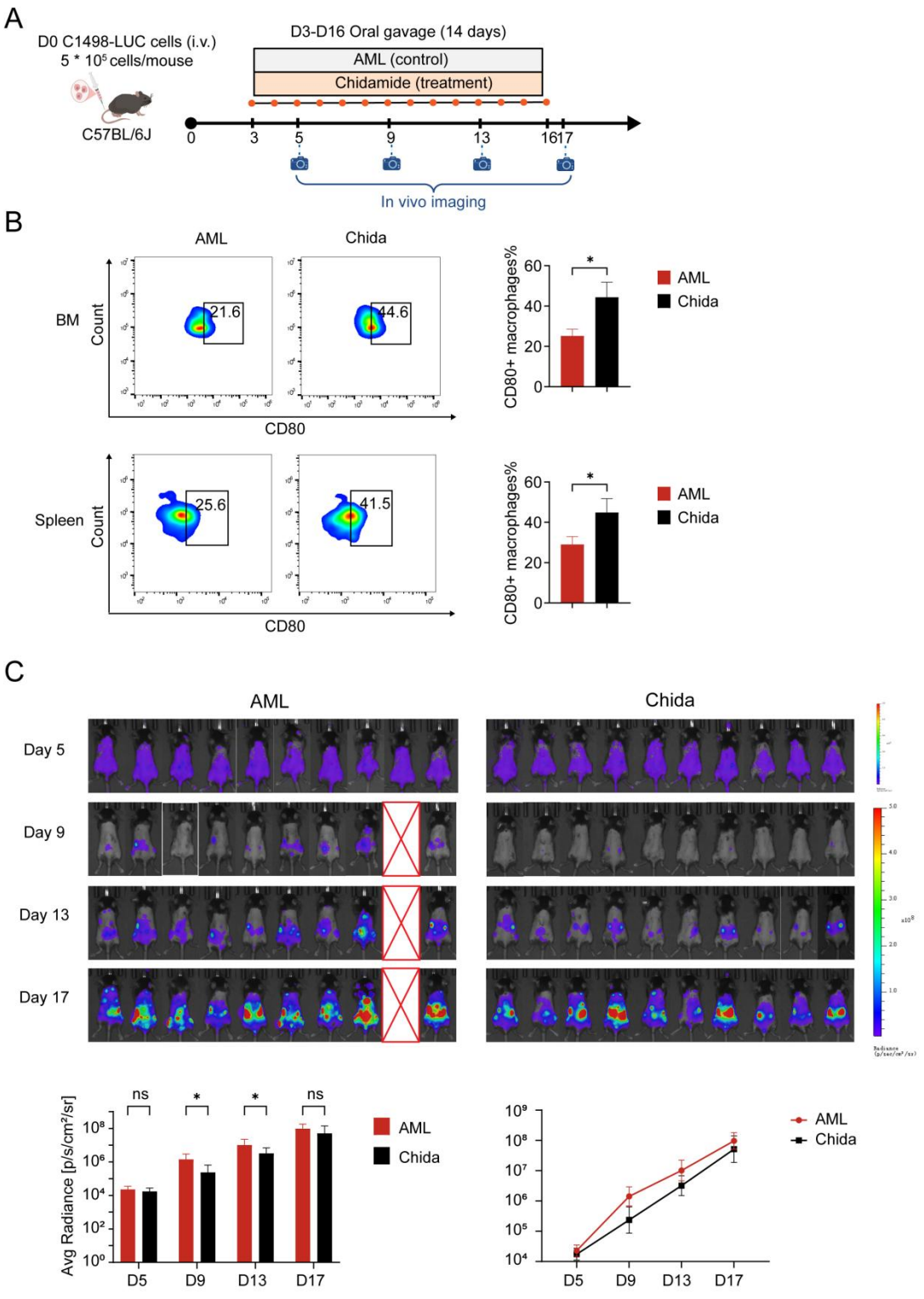


Fig. 3 Chidamide reduced leukemia burden and increased the proportion of CD80⁺ macrophages in C1498-LUC leukemia-bearing mice. **A** Schematic of the experimental design. C57BL/6 mice were intravenously injected with 5 × 10^5 C1498-LUC cells on day 0 and administered vehicle or chidamide (25 mg/kg) by oral gavage once daily from days 3 to 16. In vivo bioluminescence imaging was performed on days 5, 9, 13, and 17. **B** Representative flow cytometry plots and quantification of CD80⁺ macrophages in BM and spleen of mice treated with vehicle or chidamide

(n =3). Numbers within the gates indicate the percentages of $CD80^+$ cells within the macrophage population. **C** Representative longitudinal bioluminescence images and quantification of average radiance in vehicle- and chidamide-treated mice on days 5, 9, 13, and 17 (n = 10 biologically independent mice per group). *$p < 0.05$, **$p < 0.01$, ***$p < 0.001$; ns, not significant by paired Student's *t*-test **B-C**

the bone marrow and spleen, which coincides with reduced leukemia burden in this syngeneic AML model.

Chidamide activates the anti-tumor immunity of AAMs by inhibiting HDAC3 and enhancing H3K27 acetylation

Chidamide is a broad-spectrum HDAC inhibitor that selectively targets HDAC1, HDAC2, HDAC3, and HDAC10. To pinpoint the specific molecular target responsible for chidamide-mediated AAMs immune activation, we treated AAMs with a panel of selective HDAC inhibitors and target-specific siRNAs for functional verification. As shown in Fig. 4A-E, only pharmacological inhibition of HDAC3 via RGFP966 markedly upregulated the expression of the antigen-presenting marker CD80 in AAMs, whereas inhibitors targeting other HDAC subtypes exerted no obvious activating effects. These preliminary results suggest that HDAC3 is the key functional target by which chidamide triggers immune and inflammatory activation in AAMs. We further validated this finding via siRNA-mediated HDAC3 knockdown, which consistently elevated CD80 expression in AAMs (Fig. 4F). Furthermore, qRT-PCR and Western blot assays confirmed that chidamide treatment significantly downregulated HDAC3 expression at both the mRNA and protein levels in AAMs (Fig. 4G).

Given that HDAC3 predominantly mediates global histone deacetylation to repress transcriptional activity, we next examined the global acetylation levels of classic histone modification sites in chidamide-treated AAMs. Notably, chidamide treatment

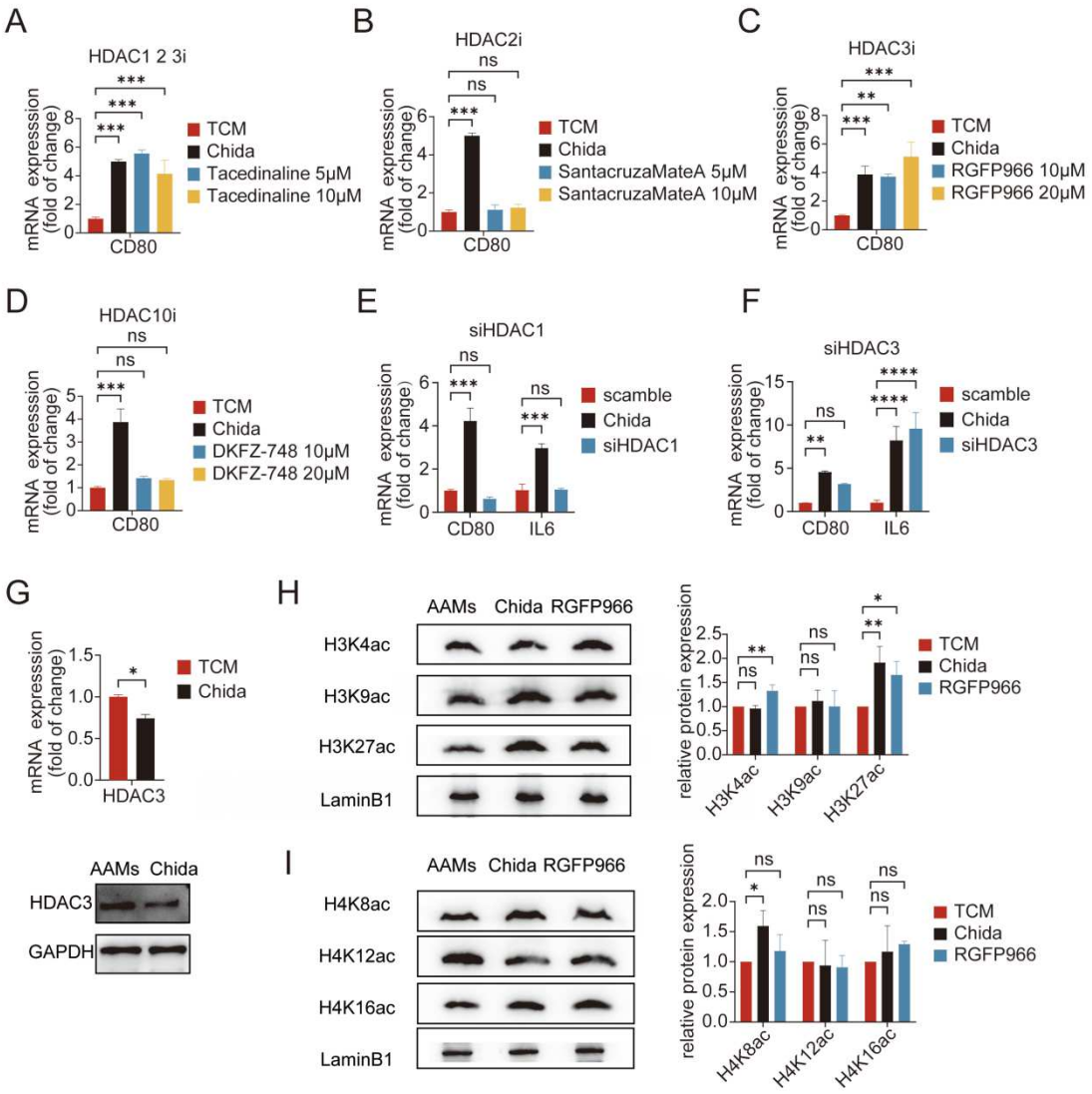


Fig. 4 Chidamide enhances AAMs function by inhibiting HDAC3 and increasing H3K27 histone acetylation levels. **A-D** AAMs were treated with specific inhibitors of HDAC1, 2, 3 (**A**), HDAC2 (**B**), HDAC3 (**C**), and HDAC10 (**D**), respectively, and *CD80* mRNA expression was detected by qRT-PCR. **E-F** HDAC1 or HDAC3 was knocked down in AAMs using siRNA technology, with or without chidamide treatment, and the mRNA expression of *CD80* and *IL-6* was measured. **G** HDAC3 expression was decreased at both the mRNA and protein levels in AAMs following chidamide treatment. **H-I** AAMs were treated with chidamide or RGFP966, respectively, and the protein expression of H3K4ac, H3K9ac, H3K27ac, H4K8ac, H4K12ac, and H4K16ac was detected by western blot. *$p < 0.05$, **$p < 0.01$, ***$p < 0.001$; ns, not significant by paired Student's *t*-test **G** or one-way ANOVA with Dunnett's multiple comparisons test **A-F, H-I**

significantly elevated global H3K27 acetylation. Although the acetylation levels of other histone residues, including H3K4, H3K9, H4K8, H4K12, and H4K16, exhibited

mild fluctuating changes, no statistically significant differences were observed between the control and chidamide groups (Fig. 4H-I). Collectively, these data demonstrate that chidamide specifically targets and inhibits HDAC3, leading to a marked increase in global H3K27 acetylation. This epigenetic alteration further facilitates the transcription of immune-related genes and ultimately potentiates the anti-tumor immune function of AAMs.

Chidamide triggers AAMs polarization and inflammatory activation via the TNF-α/NF-κB signaling pathway

To explore the downstream signaling mechanisms by which chidamide remodels AAMs, we performed transcriptomic profiling of RAW264.7-derived AAMs with or without chidamide intervention. RNA-seq analysis identified 3,949 upregulated and 1,514 downregulated genes after chidamide treatment (Fig. 5A). KEGG enrichment revealed prominent enrichment of immune- and inflammation-associated pathways, among which the TNF signaling pathway was highly ranked (Fig. 5B). Given the well-established role of the TNF-α/NF-κB cascade in driving macrophage pro-inflammatory activation and M1 polarization, we further focused on this pathway. GSEA confirmed significant activation of the TNF-α/NF-κB signature in chidamide-treated AAMs (Fig. 5C). Consistently, DoRothEA-based transcription factor activity prediction indicated enhanced activity of core NF-κB components, including NF-κB1 and RelA, following chidamide stimulation (Supplementary Fig. 4A–S4B). To validate these bioinformatic findings, qRT-PCR verified the upregulated transcription of key TNF-α/NF-κB pathway genes, including *TNF-α*, *NF-κB*, *CXCL3*, *LRF1*, and *TNFAIP3* (Fig. 5D).

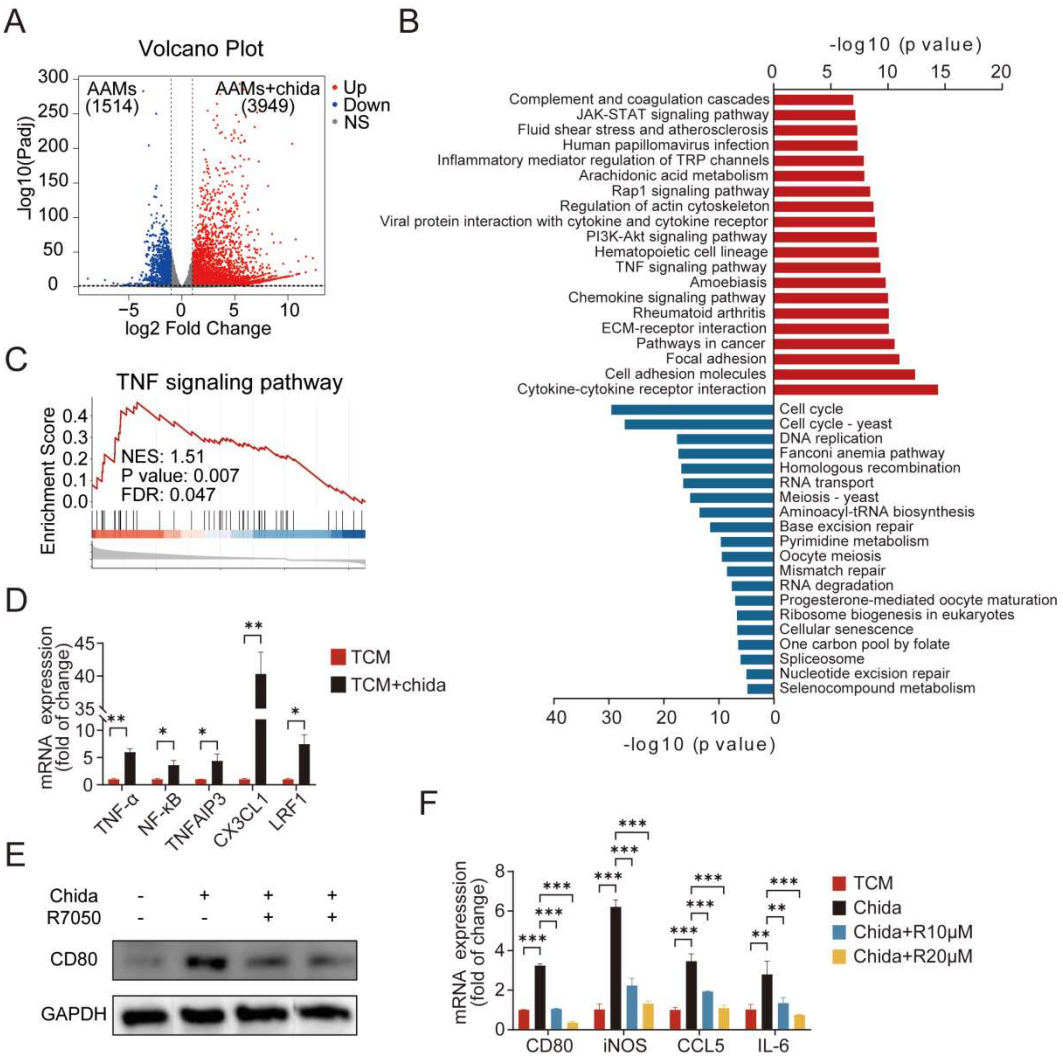


Fig. 5 Chidamide activates immune and inflammatory responses in AAMs via the TNF-α/NF-κB pathway. **A** Volcano plot showing differentially expressed genes (DEGs) in AAMs following chidamide treatment. **B** Bidirectional bar plot displaying KEGG enrichment analysis of the DEGs. **C** GSEA of the TNF-α signaling pathway. **D** qRT-PCR validation of chidamide-activated TNF-α/NF-κB pathway. **E-F** After TNF-α inhibition (R7050: 10, 20 μM), the chidamide-induced reprogramming of AAMs was reversed. $*p < 0.05$, $**p < 0.01$, $***p < 0.001$; ns, not significant by paired Student's *t*-test **D** or one-way ANOVA with Dunnett's multiple comparisons test **F**

To functionally validate whether the TNF-α/NF-κB pathway is required for chidamide-mediated AAMs reprogramming, we pharmacologically blocked TNF-α signaling using R7050 prior to chidamide treatment. Inhibition of TNF-α largely abrogated the chidamide-induced upregulation of pro-inflammatory and M1 marker genes (*CD80*,

iNOS, *CCL5*, *IL-6*), accompanied by a marked reduction in CD80 protein expression (Fig. 5E-5F). Collectively, these results demonstrate that the TNF-α/NF-κB signaling pathway is essential for chidamide-driven immune activation and pro-inflammatory polarization of AAMs.

Multi-omics analysis identifies FOSL2 as a key mediator of chidamide-induced TNF-α/NF-κB activation in AAMs

To elucidate the epigenetic mechanism by which chidamide remodels AAMs immune function, we integrated ATAC-seq, H3K27ac CUT&Tag-seq, and RNA-seq datasets to screen for key regulatory molecules. ATAC-seq analysis revealed widespread changes in global chromatin accessibility following chidamide treatment. Consistent with our earlier results, H3K27ac CUT&Tag-seq further confirmed that chidamide increased H3K27ac enrichment predominantly at gene promoter regions, indicative of transcriptionally activated chromatin status (Fig. 6A). Integrated multi-omics screening identified 265 overlapping genes characterized by elevated transcription, increased chromatin accessibility, and enhanced H3K27ac modification in chidamide-treated AAMs (Fig. 6B). KEGG enrichment analysis showed that these overlapping genes were primarily enriched in inflammatory response and TNF signaling pathways, further supporting the pro-inflammatory and immunomodulatory effects of chidamide on AAMs (Fig. 6C).

To pinpoint the core transcription factors bridging HDAC3-mediated H3K27ac remodeling and downstream inflammatory gene activation, we intersected the 265 candidate genes with a mouse transcription factor database. Eleven candidate

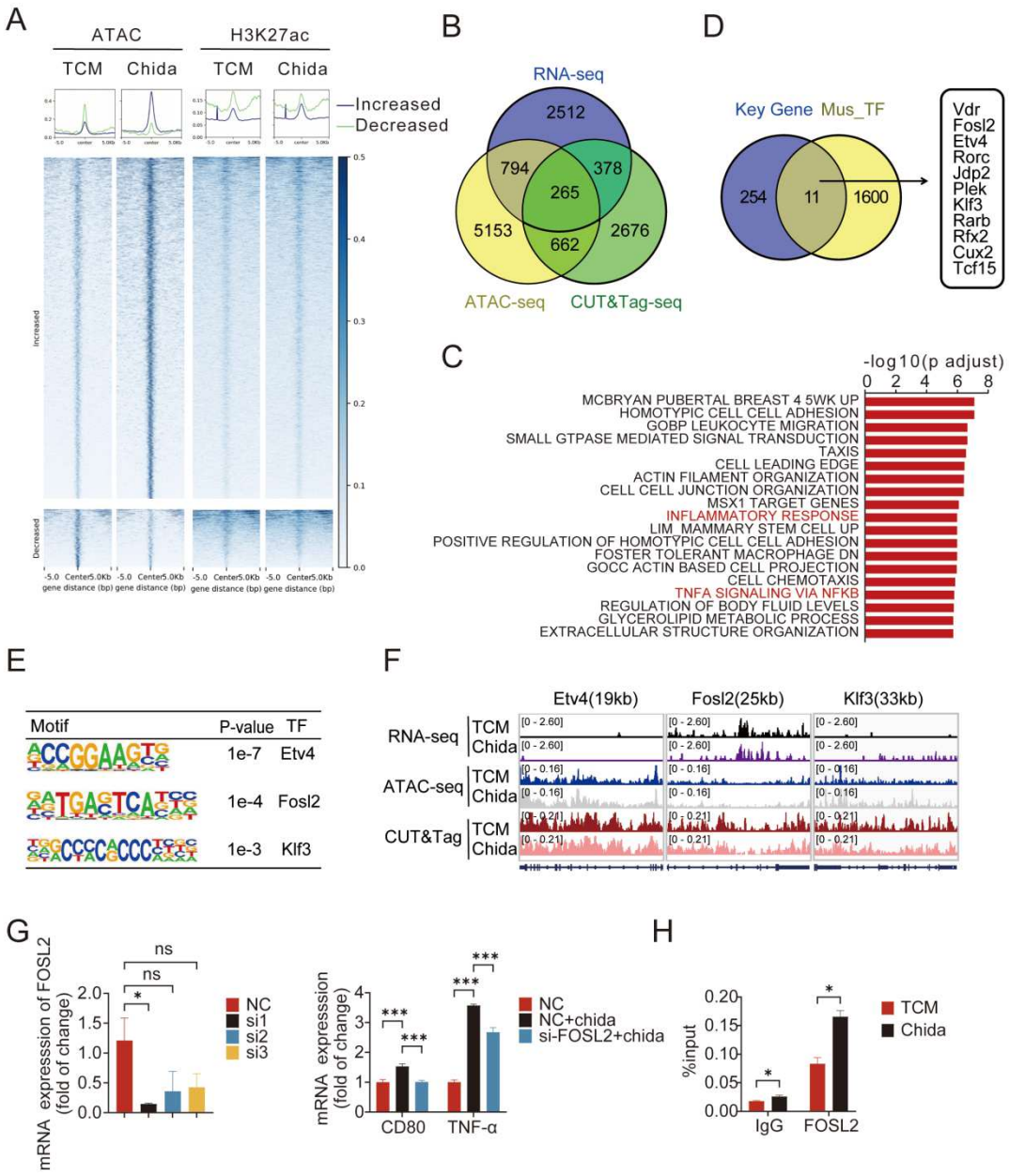


Fig. 6 Multi-omics analysis reveals the epigenetic regulatory mechanism by which chidamide activates the TNF-α signaling pathway in AAMs. **A** Heatmap showing ATAC-seq or CUT&Tag-seq coverage at sites with differential chromatin accessibility or altered H3K27ac modification in chidamide-treated AAMs compared with controls. **B** Venn diagram showing 265 genes identified in chidamide-treated AAMs that simultaneously exhibited upregulated mRNA expression (RNA-seq), increased chromatin accessibility (ATAC-seq), and higher H3K27ac levels (CUT&Tag-seq). **C** KEGG pathway enrichment analysis of the 265 DEGs, FDR < 0.05. **D** Overlap of upregulated genes between the mouse transcription factor library and the multi-omics data from chidamide-treated AAMs. **E** Motif enrichment plots of three transcription factors among the 265 overlapping genes shown in **D**. **F** Genome browser tracks (IGV plots) showing RNA-seq, ATAC-seq, and H3K27ac CUT&Tag-seq peaks at the genomic loci of ETV4, FOSL2, and KLF3. **G** FOSL2 was knocked

down in AAMs using siRNA, with or without chidamide treatment, and the mRNA expression of CD80 and TNF-α was detected. **H** ChIP-qPCR demonstrating direct binding of FOSL2 to the promoter of the TNF gene. *$p < 0.05$, **$p < 0.01$, ***$p < 0.001$; ns, not significant by paired Student's *t*-test **H** or one-way ANOVA with Dunnett's multiple comparisons test **G**

transcription factors with significantly enhanced chromatin accessibility and transcriptional activity were screened out, among which *Etv4*, *Fosl2*, and *Klf3* were the most prominent (Fig. 6D-F). Functional annotation indicated that ETV4 and KLF3 are primarily involved in non-inflammatory physiological processes and have limited relevance to macrophage activation. In contrast, FOSL2, a core subunit of the AP-1 complex, is well established as a central regulator of inflammatory transcription programs. We therefore focused on FOSL2 as the key downstream effector of chidamide-mediated epigenetic regulation.

Functional validation showed that FOSL2 knockdown largely abrogated chidamide-induced AAMs immune activation (Fig. 6G), confirming that FOSL2 is required for chidamide-mediated reprogramming. Mechanistically, ChIP-qPCR results further demonstrated that FOSL2 directly binds to the promoter region of the *Tnf* gene upon chidamide stimulation (Fig. 6H). Thus, chidamide-mediated HDAC3 inhibition and H3K27 hyperacetylation transcriptionally upregulate FOSL2 expression; elevated FOSL2 subsequently initiates *Tnf* transcription, triggering downstream TNF-α/NF-κB signaling activation and ultimately driving pro-inflammatory polarization of AAMs.

Discussion

The five-year survival rate for AML patients remains below 30%, and disease relapse accounts for most deaths, rendering AML treatment a substantial clinical challenge[30]. Leukemic relapse is tightly linked to remodeling of the bone marrow into an

immunosuppressive niche, which facilitates tumor immune evasion. Tumor-associated macrophages (TAMs) constitute a major cellular component of this suppressive microenvironment; reprogramming TAMs toward an immune-activated phenotype represents a promising strategy to counter immune escape, yet drug development targeting this approach remains limited[31, 32]. Here, we show that in macrophages within the AML microenvironment, chidamide selectively inhibits HDAC3 and elevates H3K27 acetylation, which triggers the TNF-α/NF-κB signaling cascade, reprograms AAMs into an immune-activated state, and strengthens $CD8^+$ T-cell function.

Chidamide is an orally administered selective HDAC inhibitor approved in China for relapsed/refractory peripheral T-cell lymphoma and previously untreated MYC/BCL2 double-expressing diffuse large B-cell lymphoma, with activity against HDAC1, HDAC2, HDAC3 and HDAC10. Accumulating evidence indicates that chidamide remodels the tumor immune microenvironment by boosting $CD8^+$ T-cell infiltration and effector function as well as NK cell cytotoxicity[23, 24]. In non-small cell lung cancer, chidamide blocks MDSC migration and reverses their immunosuppressive features. In lymphoma and small-cell lung carcinoma, chidamide enhances antitumor immunity by driving M1-like macrophage polarization[23, 33, 34]. Notably, the biological functions of individual HDAC isoforms are highly context-dependent across different tumor types[35, 36]. However, the regulatory effects and mechanisms of chidamide on macrophages in AML remain unclear. We demonstrate that chidamide increases expression of the M1 marker CD80 in AAMs and induces a broad panel of immune-

and inflammation-associated molecules. By reshaping AAMs function, chidamide indirectly promotes $CD8^+$ T-cell proliferation and augments antitumor immune responses. Importantly, this immune-activating effect was recapitulated in primary bone marrow macrophages isolated from patients with AML.

Mechanistically, RNA-seq identified robust enrichment of the TNF-α/NF-κB signaling axis in chidamide-treated AAMs. TNF-α is predominantly produced by monocytes and macrophages; upon binding to TNFR1 and TNFR2, it engages downstream cascades including NF-κB to control inflammatory gene transcription[37, 38]. Liu et al. previously reported that chidamide promotes M1 macrophage polarization in small-cell lung cancer via the STAT4/CCL2 axis[34]. Our work reveals for the first time that chidamide engages the canonical TNF-α inflammatory pathway in AAMs, offering new mechanistic insights into chidamide-mediated macrophage reprogramming.

Our work reveals for the first time that chidamide engages the canonical TNF-α inflammatory pathway in AAMs, offering new mechanistic insights into chidamide-mediated macrophage reprogramming[39–41]. Prior work has documented FOSL2 activity within tumor immune microenvironments. In lung cancer and triple-negative breast cancer, FOSL2 modulates TAM function and generally favors an immunosuppressive macrophage phenotype[42]. In contrast, our study is the first to demonstrate that chidamide stimulation enables FOSL2 to directly bind the *Tnf* promoter, transcriptionally inducing TNF-α expression and initiating downstream inflammatory signaling. This observation highlights that FOSL2-mediated macrophage regulation is context-dependent, shaped by the disease microenvironment and upstream

stimuli, and adds a new layer to our understanding of chidamide's epigenetic mechanisms.

This study has several limitations. First, our evidence that chidamide-reprogrammed AAMs promote $CD8^+$ T-cell proliferation and effector function derives mainly from in vitro co-culture assays; we did not further dissect how these macrophages modulate other T-cell effector programs. Second, our in vivo experiments relied primarily on a syngeneic AML cell-line model. We have not evaluated chidamide's therapeutic efficacy or its effects on the immune microenvironment using patient-derived xenograft models, which more closely recapitulate human AML.

In summary, this study systematically demonstrates for the first time that chidamide selectively inhibits HDAC3, increases H3K27 acetylation, and upregulates the key transcription factor FOSL2 to activate the TNF-α/NF-κB pathway. This cascade reprograms immunosuppressive AAMs toward an immune-activated phenotype and promotes $CD8^+$ T-cell proliferation. These findings expand our knowledge of chidamide's immunoregulatory mechanisms in AML and provide a novel mechanistic rationale for combining chidamide with existing antileukemic therapies.

Author contributions

The author contributions according to CRediT classification are as follows: Zhili Tan and Ziyi Liang contributed to methodology and investigated the study. Zhili Tan, Ziyi Liang and Xiaoning Li curated the data. Zhili Tan, Ziyi Liang, Xiaoning Li and Yujie Zhang performed formal analysis and validated the study. Rui Huang, Yaling Zheng

and Yuhua Li administered the project. Rui Huang and Yaling Zheng performed funding acquisition and supervised the study. Zhili Tan and Ziyi Liang contributed to writing-original draft preparation. Zhili Tan, Ziyi Liang and Rui Huang contributed to writing-review and editing. All authors read and approved the final manuscript.

Funding information

This research was supported by the National Natural Science Foundation of China (82100157).

Data availability statement

The data generated during the current study are available from the corresponding author on reasonable request.

Declarations

Disclosure of potential conflicts of interest

No potential conflict of interest was reported by the authors.

Ethics approval

All animal experiments were approved by the Animal Ethics Committee of Zhujiang Hospital of Southern Medical University (LAEC-2025-044). Written informed consent was obtained from all healthy donors and AML patients prior to bone marrow fluid collection. All experiments involving human samples were conducted in accordance

with the ethical principles of the Declaration of Helsinki and were approved by the Ethics Committee of Zhujiang Hospital (2026-KY-378-01).

Consent to participate

Written informed consent was obtained from all participants.

References

1. Gottardi M, De Marchi F, Ciotti G, et al (2026) The Role of the Bone Marrow Microenvironment in the Pathogenesis of Acute Myeloid Leukemia. Biomedicines 14:1679. https://doi.org/10.3390/biomedicines14081679
2. Ocaña-Cara Á, Mutis T, Van Der Schans JJ (2025) Emerging strategies in CAR-T cell therapy for acute myeloid leukemia: overcoming heterogeneity and improving safety through dual-antigen targeting. Exp Hematol Oncol 14:135. https://doi.org/10.1186/s40164-025-00726-4
3. Venugopal S, Sekeres MA (2024) Contemporary Management of Acute Myeloid Leukemia: A Review. JAMA Oncol 10:1417. https://doi.org/10.1001/jamaoncol.2024.2662
4. Forsberg M, Konopleva M (2024) AML treatment: conventional chemotherapy and emerging novel agents. Trends in Pharmacological Sciences 45:430–448. https://doi.org/10.1016/j.tips.2024.03.005
5. Lin H, Wang T, Wei J, et al (2025) Strategic innovations: Tackling challenges of immunotherapy in acute myeloid leukemia. Chinese Journal of Cancer Research

588 37:490–504. https://doi.org/10.21147/j.issn.1000-9604.2025.04.02
589 6. Ye C, Fu S, Li J, et al (2026) The eco-evolutionary dynamics of acute myeloid
590 leukemia: From clonal games to clinical intervention. Cancer Treatment and
591 Research Communications 48:101349.
592 https://doi.org/10.1016/j.ctarc.2026.101349
593 7. Zhang Y, Lu Y, Mai L, et al (2026) Dynamic heterogeneity towards drug resistance
594 in AML cells is primarily driven by epigenomic mechanism unveiled by multi-
595 omics analysis. Journal of Advanced Research 80:487–501.
596 https://doi.org/10.1016/j.jare.2025.05.038
597 8. Ochi Y, Liew-Littorin M, Nannya Y, et al (2026) Chromatin landscape and
598 epigenetic heterogeneity of acute myeloid leukaemia. Nature 656:752–762.
599 https://doi.org/10.1038/s41586-026-10703-4
600 9. Suls T, Lion E, Van Oers F, et al (2026) Inflammatory mechanisms in the AML
601 bone marrow niche: From pathogenesis to therapy. Cytokine & Growth Factor
602 Reviews 91:99–109. https://doi.org/10.1016/j.cytogfr.2026.08.001
603 10. Yang J, Liu Q, Zhang X, et al (2025) A phase 2 study of chidamide in combination
604 with CAG and venetoclax-azacitidine in acute myeloid leukemia: Clinical safety,
605 efficacy, and correlative analysis. International Immunopharmacology
606 151:114268. https://doi.org/10.1016/j.intimp.2025.114268
607 11. Carlos JAEG, Tavares MT, Lima K, et al (2025) Enhancing venetoclax efficacy in
608 leukemia through association with HDAC inhibitors. Cell Death Discov 11:147.
609 https://doi.org/10.1038/s41420-025-02446-4

12. Li Y, Seto E (2016) HDACs and HDAC Inhibitors in Cancer Development and Therapy. Cold Spring Harb Perspect Med 6:a026831. https://doi.org/10.1101/cshperspect.a026831
13. Dang F, Wei W (2022) Targeting the acetylation signaling pathway in cancer therapy. Seminars in Cancer Biology 85:209–218. https://doi.org/10.1016/j.semcancer.2021.03.001
14. Lee J, Diederich M (2026) Histone deacetylase inhibitors as venetoclax-sensitising partners in acute myeloid leukaemia: Mechanisms, pharmacology and translational perspectives. British J Pharmacology bph.70641. https://doi.org/10.1111/bph.70641
15. Li Q, Wang F, Xiang X, et al (2025) Chidamide and cytarabine synergistically treat acute myeloid leukemia: inhibiting ribosome biogenesis via the MYC-RRP9 pathway. Cell Death Dis 16:601. https://doi.org/10.1038/s41419-025-07928-y
16. Gu Z, Liu Y, Jiao Y, et al (2026) HDAC3 inhibition as a therapeutic strategy in T-cell acute lymphoblastic leukemia via the TYK2-STAT1-BCL2 signaling pathway. Front Immunol 17:1752727. https://doi.org/10.3389/fimmu.2026.1752727
17. Li X, Liu B, Huang D, et al (2025) Chidamide triggers pyroptosis in T-cell lymphoblastic lymphoma/leukemia via the FOXO1/GSDME axis. Chinese Medical Journal 138:1213–1224. https://doi.org/10.1097/CM9.0000000000003214
18. Ye J, Zha J, Shi Y, et al (2019) Co-inhibition of HDAC and MLL-menin interaction targets MLL-rearranged acute myeloid leukemia cells via disruption of DNA

damage checkpoint and DNA repair. Clin Epigenet 11:137. https://doi.org/10.1186/s13148-019-0723-0

19. Li Z, Zhang J, Zhou M, et al (2022) Epigenetic therapy with chidamide alone or combined with 5-azacitidine exerts antitumour effects on acute myeloid leukaemia cells *in vitro*. Oncol Rep 47:66. https://doi.org/10.3892/or.2022.8277

20. Ma T, Yu Y, Yang S, et al (2026) Chidamide and Anlotinib act synergistically in Jurkat cells by inhibiting the Hippo signaling pathway. Biochemistry and Biophysics Reports 45:102469. https://doi.org/10.1016/j.bbrep.2026.102469

21. Chen K, Yang Q, Zha J, et al (2020) Preclinical evaluation of a regimen combining chidamide and ABT-199 in acute myeloid leukemia. Cell Death Dis 11:778. https://doi.org/10.1038/s41419-020-02972-2

22. Gu S, Hou Y, Dovat K, et al (2023) Synergistic effect of HDAC inhibitor Chidamide with Cladribine on cell cycle arrest and apoptosis by targeting HDAC2/c-Myc/RCC1 axis in acute myeloid leukemia. Exp Hematol Oncol 12:23. https://doi.org/10.1186/s40164-023-00383-5

23. Shao J, Ye Z, Shen Z, et al (2024) Chidamide improves gefitinib treatment outcomes in NSCLC by attenuating recruitment and immunosuppressive function of myeloid-derived suppressor cells. Biomedicine & Pharmacotherapy 173:116306. https://doi.org/10.1016/j.biopha.2024.116306

24. Wen T, Sun G, Jiang W, et al (2023) Histone deacetylases inhibitor chidamide synergizes with humanized PD1 antibody to enhance T-cell chemokine expression and augment Ifn-γ response in NK-T cell lymphoma. eBioMedicine 87:104420.

https://doi.org/10.1016/j.ebiom.2022.104420

25. Cui X, Wang X, Jiang N, et al (2026) Immune modulation in gastric cancer: from macrophage polarization to immunotherapy. Front Immunol 17:1711076. https://doi.org/10.3389/fimmu.2026.1711076

26. Pan J, Li B, Lau LY, et al (2026) Metabolic and epigenetic plasticity of tumor-associated macrophages shapes immunosuppressive outputs and immune checkpoint response. Biochimica et Biophysica Acta (BBA) - Reviews on Cancer 1881:189702. https://doi.org/10.1016/j.bbcan.2026.189702

27. Wang J, Yu Y, Lin F, et al (2026) β-elemene enhances the efficacy of PD-L1 inhibitor in lung cancer by reprogramming tumor-associated macrophages to M1 phenotype via suppressing FLT1/PI3K/AKT signaling. Cancer Immunol Immunother 75:177. https://doi.org/10.1007/s00262-026-04386-z

28. Chen Z, Yang H, Yang C, et al (2026) Macrophage polarization in hematologic cancers: mechanisms and therapeutic strategies. Blood Res 61:8. https://doi.org/10.1007/s44313-025-00119-w

29. Zhao L, Li X, Liu W, et al (2026) The niche–metabolism axis: reprogramming tumor-associated macrophages for precision immunotherapy. Trends in Molecular Medicine S1471491426001784. https://doi.org/10.1016/j.molmed.2026.07.008

30. DiNardo CD, Erba HP, Freeman SD, Wei AH (2023) Acute myeloid leukaemia. The Lancet 401:2073–2086. https://doi.org/10.1016/S0140-6736(23)00108-3

31. Mantovani A, Allavena P, Marchesi F, Garlanda C (2022) Macrophages as tools and targets in cancer therapy. Nat Rev Drug Discov 21:799–820.

https://doi.org/10.1038/s41573-022-00520-5

32. Wang S, Wang J, Chen Z, et al (2024) Targeting M2-like tumor-associated macrophages is a potential therapeutic approach to overcome antitumor drug resistance. npj Precis Onc 8:31. https://doi.org/10.1038/s41698-024-00522-z

33. Dai B, Wang S, Peng X, et al (2026) Spatiotemporal Sequential Delivery of Chidamide Regulates Macrophage Reprogramming in Lymphoma Microenvironment Through HDACs-STAT3 Pathway. Advanced Science 13:e02791. https://doi.org/10.1002/advs.202502791

34. Liu W, Mei T, Jiang Y, et al (2025) Chidamide suppresses macrophage-mediated immune evasion and tumor progression in small cell lung cancer by targeting the STAT4/CCL2 signaling pathway. Cancer Biol Med 1–27. https://doi.org/10.20892/j.issn.2095-3941.2024.0241

35. Zhang Q-Q, Yu C-Z, Yu F-H, et al (2026) The HDAC1 inhibitor attenuates renal ischemia–reperfusion injury via dual epigenetic modulation of p53 and macrophage NF-κB pathways. Cell Biol Toxicol 42:84. https://doi.org/10.1007/s10565-026-10202-2

36. Yu J, Yang S, Zha X, et al (2026) HDAC6 Promotes Host Defense Against Chlamydial Lung Infections by Regulating M2-Th2 Responses. IJMS 27:3009. https://doi.org/10.3390/ijms27073009

37. Aggarwal BB (2003) Signalling pathways of the TNF superfamily: a double-edged sword. Nat Rev Immunol 3:745–756. https://doi.org/10.1038/nri1184

38. Brenner D, Blaser H, Mak TW (2015) Regulation of tumour necrosis factor

signalling: live or let die. Nat Rev Immunol 15:362–374. https://doi.org/10.1038/nri3834

39. Wang Q, Martínez-Bonet M, Kim T, et al (2023) Identification of a regulatory pathway governing TRAF1 via an arthritis-associated non-coding variant. Cell Genomics 3:100420. https://doi.org/10.1016/j.xgen.2023.100420

40. Liu K, He X, Huang J, et al (2023) Short-chain fatty acid-butyric acid ameliorates granulosa cells inflammation through regulating METTL3-mediated N6-methyladenosine modification of FOSL2 in polycystic ovarian syndrome. Clin Epigenet 15:86. https://doi.org/10.1186/s13148-023-01487-9

41. Huang H, Ren Y, Liang H, et al (2021) Mechanism of TCONS_00147848 regulating apoptosis of nasal mucosa cells and alleviating allergic rhinitis through FOSL2-mediated JAK/STAT3 signaling pathway. Sci Rep 11:15991. https://doi.org/10.1038/s41598-021-94215-3

42. Hey J, Halperin C, Hartmann M, et al (2023) DNA methylation landscape of tumor-associated macrophages reveals pathways, transcription factors and prognostic value relevant to triple-negative breast cancer patients. Intl Journal of Cancer 152:1226–1242. https://doi.org/10.1002/ijc.34364

Supplementary Files

This is a list of supplementary files associated with this preprint. Click to download.

- Supplementalinformation.docx